ARMY RESEARCH LABORATORY

# Computer Study of the Ionic Mechanisms of Organophosphorous-Caused Long-QT Syndrome (LQTS)

by Csaba K. Zoltani and Steven I. Baskin

ARL-TR-2902 February 2003

## NOTICES

### Disclaimers

The findings in this report are not to be construed as an official Department of the Army position unless so designated by other authorized documents.

Citation of manufacturer's or trade names does not constitute an official endorsement or approval of the use thereof.

Destroy this report when it is no longer needed. Do not return it to the originator.

**Army Research Laboratory**
Aberdeen Proving Ground, MD 21005-5067

**ARL-TR-2902** **February 2003**

# Computer Study of the Ionic Mechanisms of Organophosphorous-Caused Long-QT Syndrome (LQTS)

**Csaba K. Zoltani**
**Computational and Information Sciences Directorate, ARL**

**Steven I. Baskin**
**U.S. Army Medical Research Institute of Chemical Defense**

## Acknowledgments

It is a pleasure to thank Dr. John Pormann from Duke University for making CardioWave available and giving expert advice on its use.

## Contents

## List of Figures

## List of Tables

# 1. Introduction

Organophosphorous (OP) compounds, ingredients in insecticides and military nerve agents, cause repolarization abnormalities of the ventricles, a precursor to the often fatal cardiac arrhythmia.

OP in the cardium is expressed by an overload of acetylcholine (ACh), lesions in the tissue and blockage of the second messenger system, the vasoactive intestinal peptide (VIP), and a peptide instrumental in increasing the heart rate. The ACh overload results from the OP binding to acetylcholinesterase (AChE) preventing the hydrolysis of ACh. But knockout murine experiments [1] as well as data from India [2] on insecticide production workers have shown that OPs can cause cardiac toxicity even in tissue that is devoid of or very low in concentration of AChE. This suggests that a complete description of OP poisoning requires the consideration of effects in addition to ACh overload. Tables 1 and 2 summarize the most important effects of OP expressed in the heart [3–8].

Kiss and Fazekas [3], Ludomirsky et al. [4], and Bar-Meir et al. [5] discuss clinical cases of OP-affected individuals that often progress from atrial bradycardia, at the onset of the poisoning, to Torsade de Pointes (TdP) that may culminate in ventricular fibrillation (VF) and sudden cardiac death (SCD). With OPs, there can be a delay of up to 2 weeks, also called the intermediate stage, before the VF manifests itself.

Changes in the electrocardiogram (ECG) provide important clues to the changes caused in the electrophysiology by the presence of OPs (Table 1). Of special significance is the lengthening of the LQT segment and the changes in the T-wave, which often becomes pointed with the maximum voltage considerably elevated. Of special significance is the elongation of the LQT since it is an indicator and predictor of ventricular fibrillation. Both the T-wave and the LQT portion of the electrocardiogram are expressions of repolarization, thus changes in these reflect repolarization anomalies. Repolarization is primarily determined by and controlled through several potassium and calcium currents. Changes in these currents have a profound effect on the cardiac cycle because the action potential is changed.

Table 2 summarizes the most important changes in the membrane currents in the presence of OP deposition. The three main effects are (1) the changes caused by the OP binding to the AChE, (2) the consequence of the lesions within the tissue, and (3) the blocking of the second messenger, the most important of which is the VIP.

According to several investigators [3–5], ~85% of OP-affected individuals exhibit the Long-QT Syndrome (LQTS) [9–11], which is a lengthening of the time needed for repolarization of the

Table 1. OP-caused ECG changes.

| QRS Complex | QT-Lengthening | ST Elevation/Depression | T-wave | P-wave | Miscellaneous |
|---|---|---|---|---|---|
| Activation of both ventricles, 120 ms | <440–460 ms | ST-T wave ventricular recovery | | Activation of atria <120 ms, PR-duration of AV conduction 120–200 ms | |
| Prolonged | Prolonged-repolarization disorder | Ischemia/infarction | Inversion | Extracellular hyperkalemia reduces wave amplitude | BP modulation |
| Hyperkalemia | $I_{Kr}\downarrow\downarrow$ | Hyperkalemia produces ST elevation | Disappearance | Reduces atrial, ventricular resting membrane potentials | Sinus bradycardia (20–30 bpm) |
| | $I_{Ks}\downarrow$ | | Narrow peaked | | Ventricular tachycardia<br><br>Torsade de Pointes (TdP) |
| | Hypocalcemia | | Changes caused by alterations in duration of ventricular, atrial action potentials | | Atrial fibrillation, AV block |
| | Hyperkalemia shortens QT interval | | Altered ventricular activation | | Ventricular fibrillation |
| | | | | | Changes in primary center of ventricular automation |

Table 2. Effects of OPs on cardiac tissue.

| Bound to AChE | Lesions | | | | Second Messenger (VIP, others) |
|---|---|---|---|---|---|
| | **Acidosis** | **Anoxia** | **Modulated Ion Concentration** | **Release of Catecholamines** | |
| ACh overload causes bradycardia, slows conduction in AV<br>Prevents hydrolysis<br>$[Ca^{++}] \uparrow \rightarrow I_{KACh} \uparrow$ | (Intracellular proton accumulation), pH $\downarrow$, $Na^+/H^+$ exchange $\uparrow$<br>$[ATP] \downarrow$<br>$[K^+]_o \uparrow$, reduces $I_{Kr}$ by increasing rate of deactivation, shifts voltage dependence of activation to more positive potentials | Lowers ATP, cAMP, cGMP, ATPase inhibition<br>$I_{K(ATP)} \uparrow$ (activated), AP shortened | $[K^+]_o \uparrow$<br>Effect on velocity of propagation, inexcitability<br><br>$[Na^+] \uparrow$<br>$Na^+/K^+$ pump inhibition<br>$Na^+/Ca^{++}$ exchanger $\rightarrow$ $Ca^{++}$ influx | Prolongs AP, $[Na^+] \uparrow$, $Na^+$ - $K^+$ ATPase antagonized<br>DAD enhanced<br>Difference for $\alpha$, $\beta$ receptors | Adenylate cyclase activation<br><br>$I_f \uparrow$, cAMP $\uparrow$, $\rightarrow$ HR $\uparrow$<br>OP reduces cAMP $\rightarrow$ $Ca^{++}$ influx, inhibits adenylate cyclase, stimulates ATP, $I_K \uparrow$, affects $I_{Ca(L)}$, EAD, DAD $\rightarrow$ arrhythmia |
| Antagonizes adenylyl cyclase | $g_K \uparrow$<br>Cytoplasmic $[Ca^{++}] \uparrow$ slows repolarization, reduces max diastolic potential | | $[Ca^{++}] \uparrow$<br>$Na^+/Ca^{++}$ exchanger $\downarrow$ reduced SR uptake<br><br>$[Mg^{++}] \uparrow$ (hydrolysis of ATP), activates enzymes<br>Reduces $I_{Ca(L)}$, $I_{K1}$, $I_{KACh}$, $I_{KATP}$, $I_{Ks}$ | Adrenergic $\alpha$ stimulation: reperfusion arrhythmia ($Ca^{++}$ overload), gap junction conductance $\downarrow$, exchanger stimulation, activates $Na^+/K^+$ pump | |
| Arrests cAMP synthesis<br>Depresses $I_f$ (pacemaker current)<br><br>ACh inhibits adenylate cyclase | $I_{Ca(L)} \downarrow$<br><br>$I_{Na} \downarrow$ (inactivation of fast $Na^+$ channel)<br>Decreased excitability<br>$CO_2$ accumulation | | | Adrenergic $\beta$ stimulation: stimulates adenylate cyclase, elevate cAMP, increase $Ca^{++}$ influx, $I_f$ activation, triggered activity improves modal conduction | |
| Intermediate Stage | | | | | |
| AF, VF | | | | | |

Notes: g = conductivity of the tissue; [..] = concentration; $I_{(.)}$ = ionic current with the subscript denoting the channel type; $\uparrow$ denotes an increase; $\downarrow$ denotes a decrease; $\rightarrow$ means yields.

ventricle. This condition has also been tied to mutations in several genes, including HERG, encoding ion channels, and can also be induced by medication (acquired LQTS). The result is modulated ion flow, an inflow of excess sodium, accumulation of calcium in the sarcoplasmic reticulum and reduced potassium outflow. The calcium ion distributions within the cells are also altered. A delayed influx of $Ca^{++}$ ions suggested Ca/K exchange and contributes to early after depolarization (EAD), thought to trigger ventricular arrhythmias.

Animal models and experimental data show that in OP-caused poisoning the slope of the onset of the depolarization, governed by the flux of the $Na^{+}$ ions, is changed. In addition, modulation of the potassium currents, $i_{Kr}$ and $i_{Ks}$ are observed. Plateau current imbalance and a blockage of the ion channel responsible for these currents are thought to be present. Under these circumstances, a prolongation of the repolarization time of the ventricles results. A repolarization lengthening by a few percent is an indicator of a precursor to arrhythmogenicity. Action potential duration (APD) lengthening enables EADs triggering focal arrhythmia.

Zeng et al. [12], working with guinea pig ventricular myocytes, found that $i_{Ks}$ is the major plateau repolarization current and that a block of either $I_{Kr}$ or $I_{Ks}$ results in abnormal repolarization. Viswanathan et al. [13] showed that the effect of the heterogeneity of $I_{Ks}$ and $I_{Kr}$ has a profound influence on action potential duration and may influence arrhythmogenesis. Differences in cardiac cell types contribute to this heterogeneity. Liu and Antzelevitch [14] found that smaller $I_{Ks}$ prolong the action potential of the midmyocardial myocytes.

The following sections describe a computer study of the effect of OP on the electrophysiology of ventricular tissue, especially the processes that favor LQTS, which subsequently may culminate in VF. Separately, this study does not address the effect of acidosis or hypoxia. Changes in the activation of muscarinic receptors are thought to be secondary to the ACh overload. In the atria, ACh overload can be associated with muscarinic responses. While in the ventricle, it may be directly coupled to $K^{+}$ ion conductance. The approach adopted is to modulate the conductivities of channels and regional ion concentrations affected by OP. The resulting change in current flow is reflected in the changed action potential dynamics.

## 2. Methods and Materials

### 2.1 The OP-Affected Tissue Characterization

Histopathological examination of cardiac tissue shows that OPs produce lesions reminiscent of ischemia. In terms of the effect on membrane electrophysiology, this translates into elevated and heterogeneous accumulation of potassium and the development of acidosis [15]. The major effect of acidosis is calcium overload of the sarcoplasmic reticulum, which may lead to

spontaneous action potential generation anywhere within the heart. In addition, very small changes in pH can substantially affect the strength of the contraction of the heart. The pH in the tissue, both intra- and extracellularly, drops linearly about 1 pH below the normal value of ~7.1. There is a significant reduction in the sodium current, $I_{Na}$, and a decrease in the resting membrane potential. $I_{Ca(L)}$ decreases in tandem due to a change in the channel conductance. The decrease in conductance, at pH = 6.6, has been estimated as 50%. The inward rectifier potassium current, $I_{K1}$ increases due to an elevation in the $[K]_o$. Sympathetic nerve catecholamine release also leads to elevated norepinephrine release.

As a consequence of anoxia, ATP declines, between 40% and 60% in value, and $I_{K(ATP)}$ channels open up and contribute to the repolarization current. $I_{K(ATP)}$ is inactive in healthy tissue. These changes are accompanied by a decline in the membrane excitability, the maximum value of the membrane voltage with respect to time. Its value is ~400 V/s but declines to about 100 V/s at $[K^+]_o = 12$ mM. In addition, increases in $Na^+$ and $Ca^{++}$ uptake take place.

There are indications that OP also blocks the second messenger route that involves the VIP [16]. This peptide is abundantly present in cardiac tissue and works as agonist of adenylate cyclase. OP block of VIP antagonizes bradycardia, one of the initial manifestations of OP-intoxication.

### 2.2 The Simulation Setup

The dynamics and integrity of the action potential propagation in OP-affected ventricular tissue, whose normal electrophysiological behavior is described by the Luo-Rudy model [17], was simulated with the modifications noted in Table 3. The simulated tissue, 3 × 3 cm in size, was represented as a slab of 300 × 300 × 1 nodes. A stimulus was applied to the left-hand edge consisting of a pulse of 200 $\mu A/cm^2$ of 2 ms in duration. The presence of OPs was modeled in the tissue varying the conductivity of selected ion channels. A possible cause is the blocking of the channels by a ligand. It should be noted that in an intoxicated tissue, OP is heterogeneously distributed in the heart and that hyperkalemia is one manifestation of OP toxicity. This is coarse graining the problem since localized sodium and calcium concentration deviations due to OP presence are also indicators of the change of the state of the cell. In addition to modulating the potassium current, OP-caused lesions in the tissue were modeled by including the effect of anoxia, simulated by modulation of calcium conductivity, and acidosis by a 25% reduction of the conductivity of the calcium and potassium channels, Table 3. Pacing was used to ensure stable initial conditions.

Initially, a baseline calculation, using the parameters of Table 4, was performed. The ion concentrations were those of a normal tissue. In succeeding runs, to simulate the effect of OP toxicity, the parameters shown in Table 3 were varied.

Table 3. Parameters for simulation of the effect of OP toxicity.

| Parameter | Change from Luo and Rudy [17] Noted | |
|---|---|---|
| | **Computer Experiment No. 1** | **Computer Experiment No. 2** |
| $g_{Na}$ | ↓ | |
| $g_K$ | ↓ | |
| $g_{Ca}$ | | ↑ |
| $g_b$ | (reformulated in Luo and Rudy [17]) | ↓ |
| $[K^+]_i$ | ↑ | |
| $[Ca^{++}]_i$ | ↑ | |

## 3. Simulation

The model of the ventricular action potential used in these calculations is the Luo-Rudy model [17] extending the earlier Beeler-Reuter formulation using guinea pig experimental data. The version adopted here simplifies the model in that the potassium currents are not split into fast and slow components but the earlier composite version is used. Intracellular calcium processes were not tracked in these calculations, but the overall calcium level, which has an effect on the resting voltage, was modulated. Assuming the cardiac tissue to be a continuum, the action potential was tracked through the domain according to the cable equation, a second-order partial differential equation. It relates the temporal change in membrane voltage V to the spatial change and the $I_{ion}$, the transmembrane ionic current, describing the sodium, potassium, calcium and chloride currents, pumps, and exchangers. $D$ is the diffusion constant and $C_m$ the membrane capacitance. A value of 1 $cm^2/s$ was used for $D$ and $1\mu F/cm^2$ for the capacitance. In the calculations fiber orientation (one of the diffusion matrix entries) was assumed to be uniform. Additional equations describe the gating variables of the ionic channels and the change of the ion concentrations. No flux boundary conditions were used.

The calculations were carried out with the code CardioWave on the computer assets of the Major Shared Resource Center at Aberdeen Proving Ground, MD.

Table 4. Simulation parameters.

| | Present Study | Remarks |
|---|---|---|
| Conductivity (mS/F) | | |
| $g_{Na}$ (sodium channel) | 16.0 | |
| $g_K$ (potassium channel) | $0.282([K^+]_o/5.4)^{0.5}$ | function of $[K^+]_o$ |
| $g_{K1}$ (time indep potassium channel) | 0.75 | |
| $g_{kp}$ (plateau) | 0.00552 | Zeng et al. [12] |
| $g_{Ca}$ (calcium channel) | 0.09 | |
| $g_b$ (background) | 0.04 (formerly) | no longer used in Luo and Rudy [17]) |
| Reversal potential (mV) | | |
| $E_{Na}$ | 54.4 | |
| $E_K$ | −77.0 | |
| $E_{K1}$ | −87.26 | |
| $E_b$ | −59.87 | |
| $E_{Ca(L)}$ | $\sim\ln[Ca^{++}]_i$ | |
| Gating parameters | | |
| m | 0.0008 | changed from original formulation |
| h | 0.9937 | |
| j | 0.9957 | |
| d | 0.00000321 | changed from original formulation |
| f | 0.99998 | |
| x | 0.029838 | |

In parallel mode, a typical calculation on 16 nodes of the SGI Origin 3000* server, with 300-MHz IP27 processors and data cache size of 32 Kb, required 7 hr and 15 min nondedicated time. This time was improved with a larger number of processors, but the speedup was not linear (Table 5).

Table 5. Wall-clock time required on the SGI Origin 3000 server for a 300 × 300 node calculation.

| Number of Processors | Nondedicated Wall Clock Time |
|---|---|
| 16 | 7 hr 15 min |
| 32 | 4 hr 11 min |
| 64 | 2 hr 8 min |

## 4. Results

The effect of the presence of OP in the cardiac tissue was simulated by modulating channel conductivities and ion concentrations. The action potential data, unless noted otherwise, is from a location, picked at random, located at 0.02 cm horizontally and 0.05 cm longitudinally from the left edge of the tissue. For the parameters used, the baseline cycle length was 400 ms, and the conduction velocity was 60 cm/s. The plateau, representing the repolarization, extended from 50 to 300 ms, followed by a steep decline to the resting voltage of −84.0 mV.

Figure 1 shows the effect of changing the potassium channel conductivities to one-tenth the normal value. The action potential shows considerable cycle lengthening when contrasted with the baseline. At 500 ms, the voltage is −18 mV, still far from the resting value. The slope of the action potential curve indicates that considerable time will elapse before the voltage drops to the initial state. The effect on the action potential of the reduction in conductivity of the potassium ion channels is shown in Figure 2. The lower trace is the baseline, and proceeding vertically, the curves represent 80%, 60%, and 40% values of the baseline channel conductivity. Already a 20% reduction in conductivity lengthens the cycle by close to 10%. At 40% a 100 ms increase in

* SGI Origin 3000 is a registered trademark of Silicon Graphics, Inc.

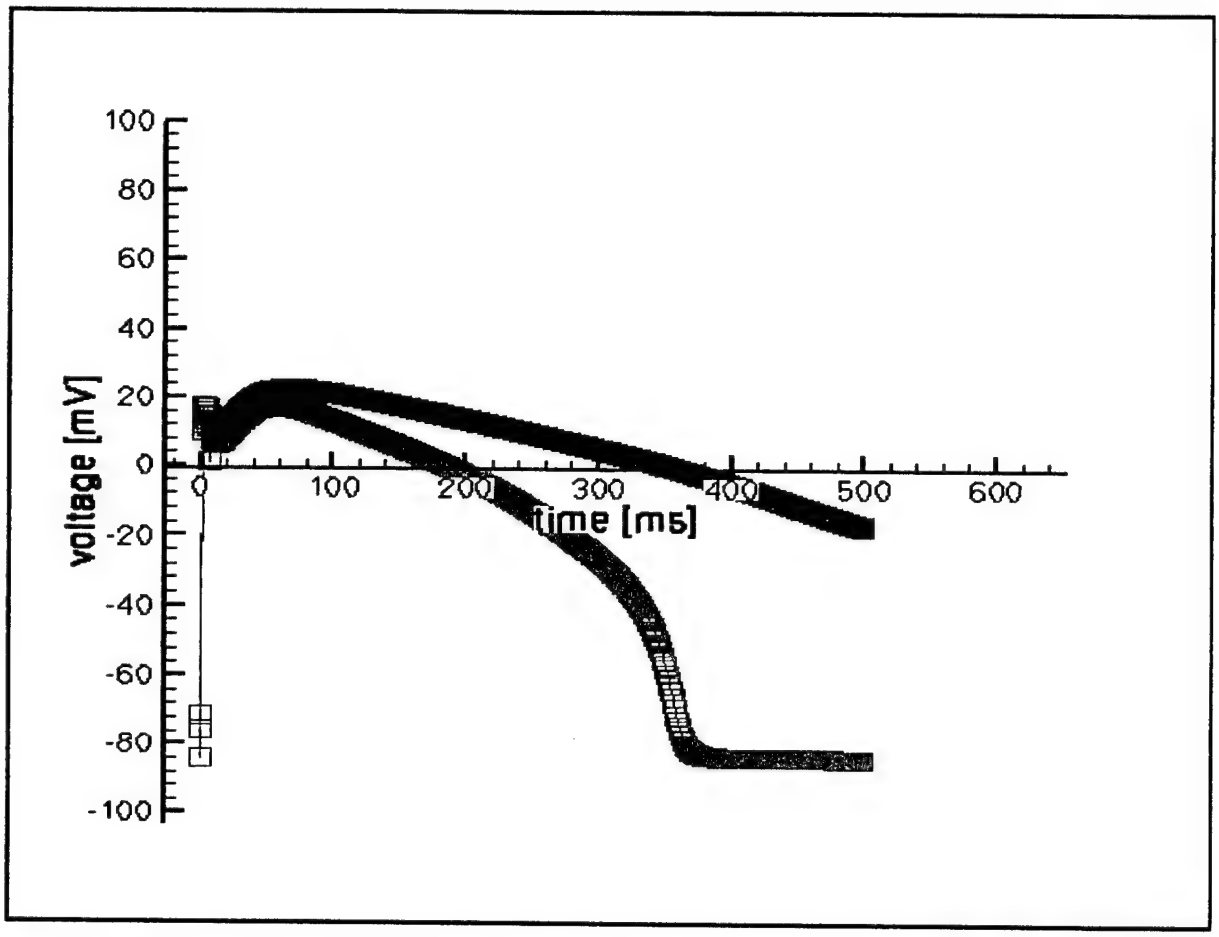


Figure 1. The baseline behavior (lower trace) of the ventricular action potential contrasted with the reduction in potassium channel conductivity to 10% of control (upper trace). Data points were included for emphasis of the lengthening of the cycle.

the cycle length is noted. At 60% more than doubling occurs. There is also an 8% decline in the slope of the depolarization when the potassium channel conductivity is lowered to 10% of baseline. Figure 3 shows that when both $g_K$ and $g_{K1}$ conductivities are reduced by 60%, the cycle length becomes indeterminate. A calculation extended to 1000 ms shows that the voltage oscillates in the negative voltage range and does not return to the resting state (Figure 4). This behavior mimics Tdp, a precursor to VF.

Increasing the Ca/K exchange current by doubling the channel conductivity more than doubled the peak of the potential voltage and extended the cycle time by several hundred milliseconds. When the background conductivity was doubled, the action potential oscillated in the negative voltage range, reaching only −20.0 mV (Figure 5). Cycle lengthening (not shown) was also observed when the $g_{K1}$ was lowered to 0.1; indeed, a 25% increase was noted.

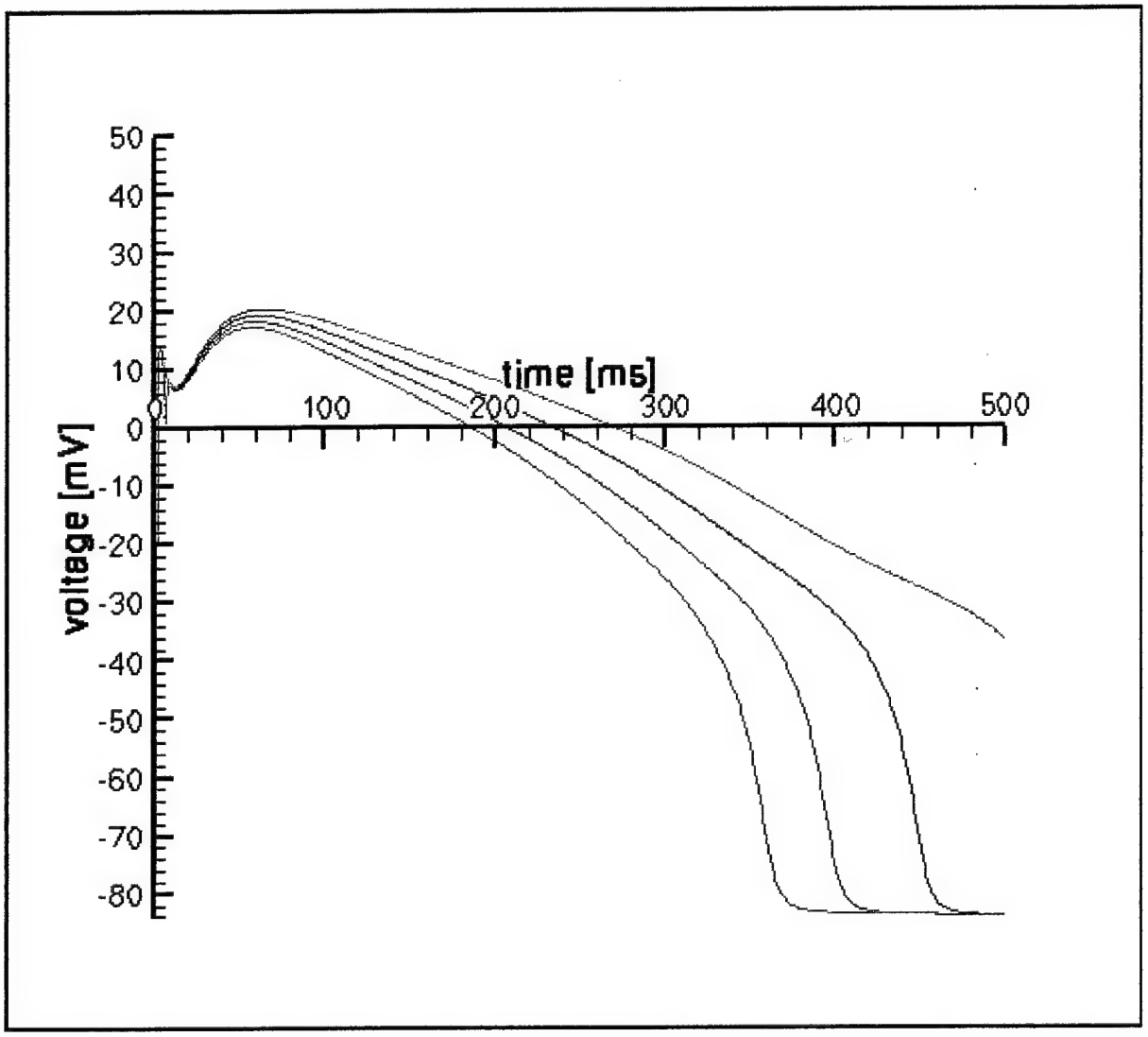


Figure 2. Action potential of the ventricular tissue at various values of the potassium channel conductivity. The baseline is the lowest curve and proceeding upward, the corresponding curves are at 80%, 60%, and 40% values of the conductivity. The cycle lengthening is apparent.

The effect of lowering the background current is shown in Figure 6. The cycle length increase to 480 ms (an increase of ~37%). Separately increasing the inward calcium flow (upper trace) results in an indeterminate lengthening of the cycle length, a probable shutdown of the heart. Decreasing the background current by adjusting the conductivity to one-tenth the normal value had two effects: the maximum value of the depolarized voltage approached 50.0 mV, and the cycle lengthened to 500 ms. The repolarization plateau showed a gradual decline, with a precipitous drop from −25.0 to −84.0 mV commencing at 450 ms into the cycle.

Figure 6 reinforces the observation that a calcium overload, twice the normal concentration and typical of OP-caused condition, in this case in tandem with potassium channel conductivity reduction, considerably expands cycle length, and probably shuts down the heart.

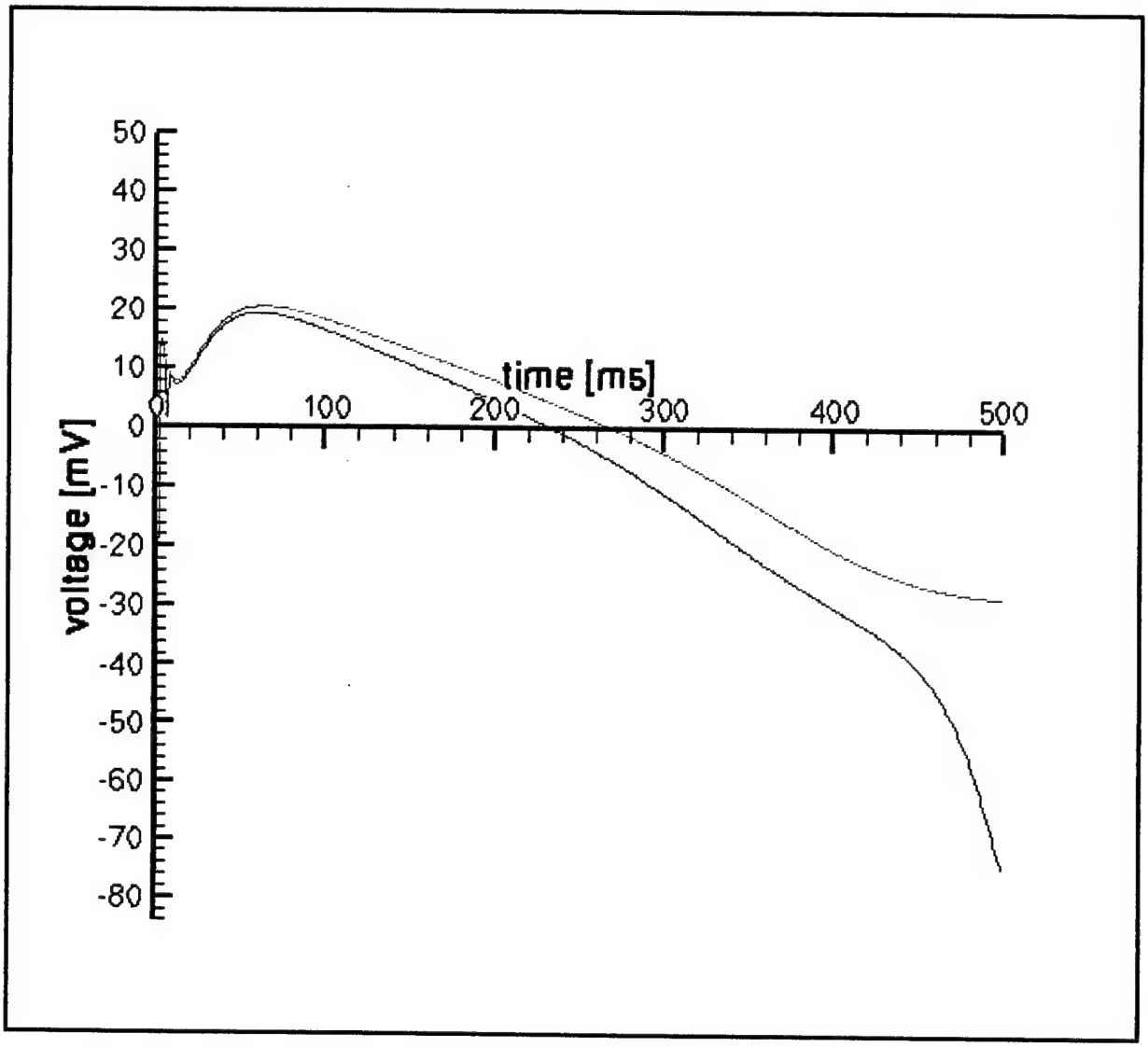


Figure 3. The effect of lowering both the $g_K$ and the $g_{K1}$ conductivity to 60% (lower curve) and 40% (upper curve). Significantly, the reduction to 40% results in the action potential unlikely returning to the rest state, thus there is a cessation of electrical activity of the ventricle.

With anomalously increase $Na^+$ and $Ca^{++}$ concentrations and thus background current, the action potential stays in the negative domain, as shown in Figure 7. The second stimulus, of the same magnitude as the first one, has a considerably shortened cycle length and plateau. The potassium current that is fully activated at +10 mV has been affected. Here the effect of the increased sodium ions seems to outweigh the effect of the calcium ions that is known to enhance the potassium current in a dose-dependent fashion [18].

Reentry arrhythmia was observed when a second stimulus, perpendicular to the initial one, was launched at 425 ms (Figures 8 and 9). It should be noted that the second wave propagated transversally much faster in portions of the tissue that had longer to recover. The characteristic spiral presaging reentry was observed at the head of the wave front.

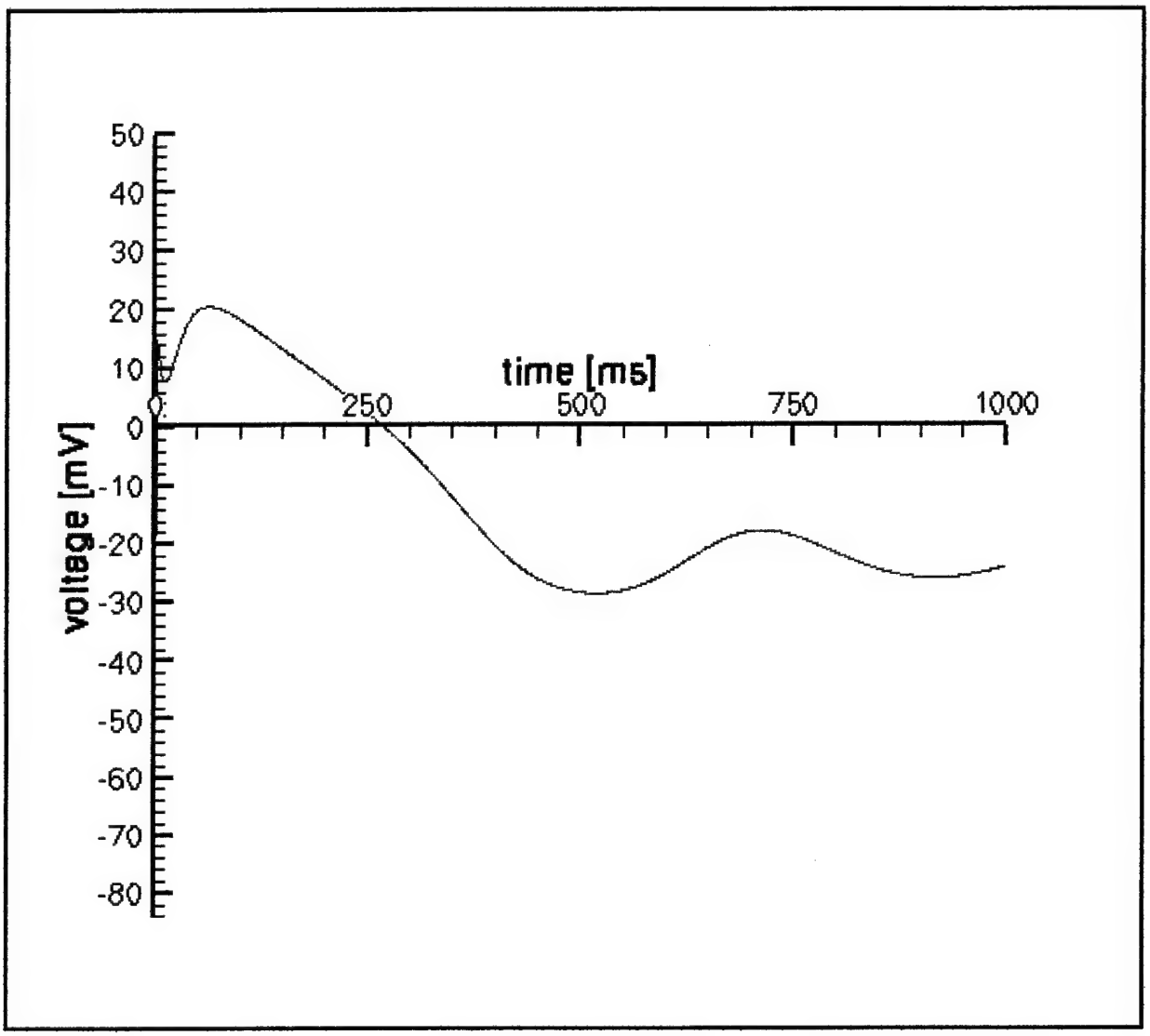


Figure 4. With a 40% value of the $g_{K1}$ and $g_K$, the action potential does not return to the resting state. This data gives an appearance of TdP activity.

We propose an estimated dose-response curve (Figure 10) based on the observation that the probability of the onset of fibrillation is directly related to, though not exclusively dependent upon, the flow of potassium ions, i.e., the conductivity of the channel. The OP-caused reduction of the conductivity is reflected in the prolongation of the repolarization. A prolongation of 10% of QT of the ECG is a predictor of fibrillation, thus the corresponding channel conductivity is related to the lethal dosage. Analogously, the estimated onset of TdP and tachycardia correspond to lesser conductivity changes, i.e., cycle prolongation.

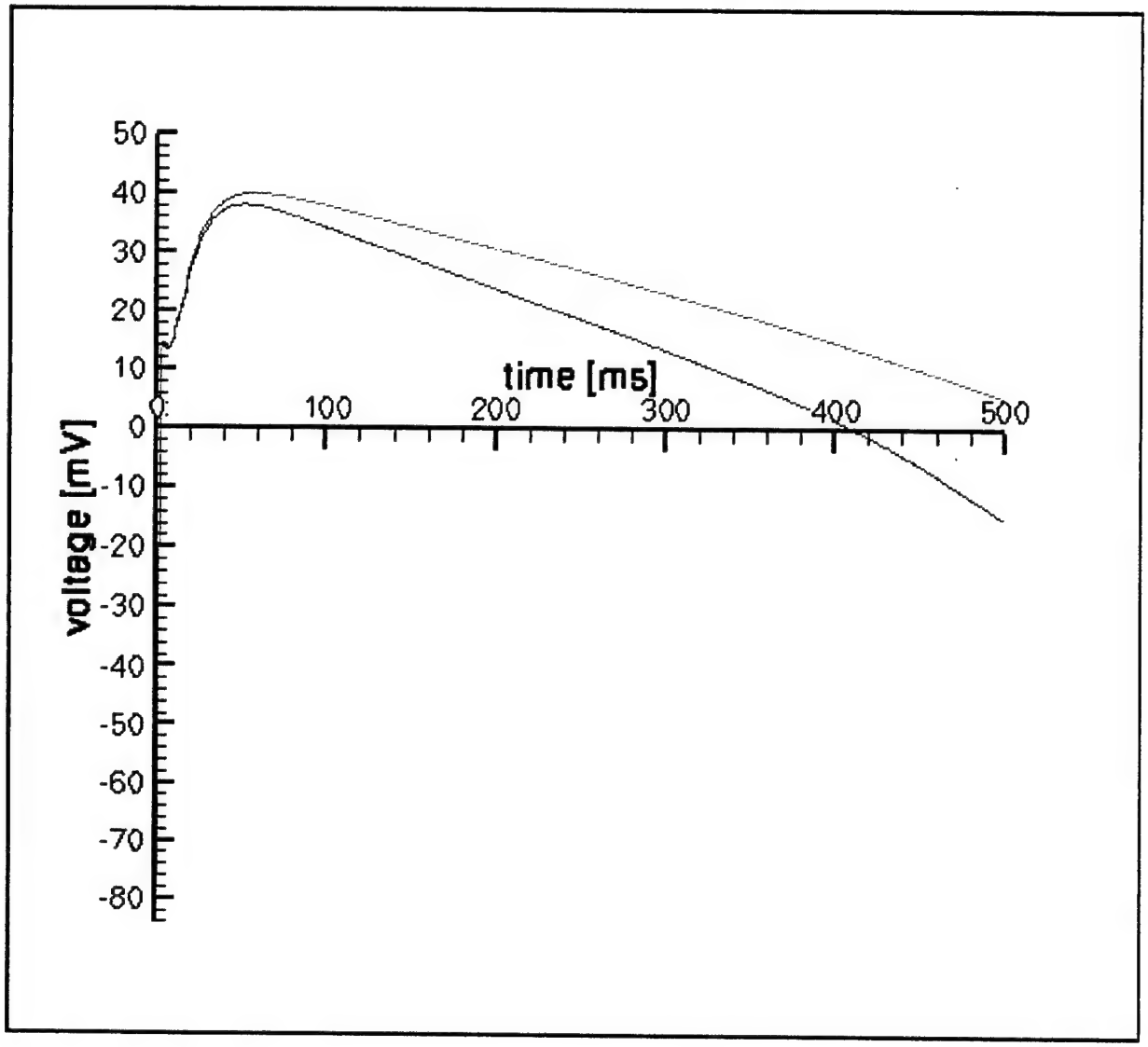


Figure 5. The effect of the calcium overload (twice normal, typical of OP-caused condition) while the potassium channel conductivity is lowered to 60% (lower) and 40% (upper) curve. In the latter case, the ventricle ceases to function.

## 5. Discussion

Animal experimental data show that OP intoxication results in lesions of the cardiac tissue, acidosis, and anoxia. These effects in terms of the membrane currents can be expressed and simulated by ion channel conductivity changes. Potassium conductivity changes, which can be caused by ligand blocking the channel, are major contributors to increased cycle length and, consequently, LQTS. Modulating the channels that are affected by OP, LQTS can be simulated. It is clear that LQTS is a precursor to reentry and the onset of fibrillation.

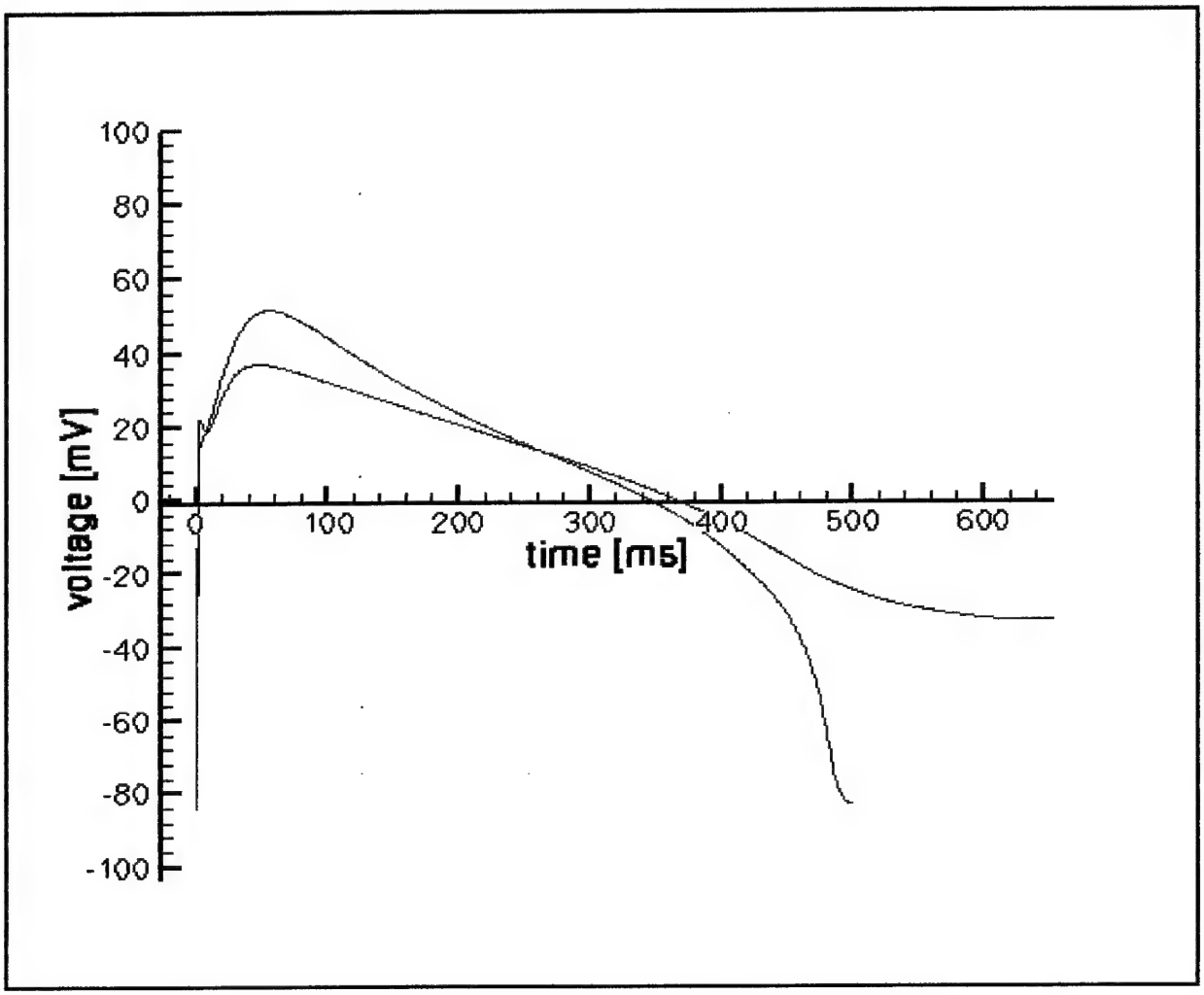


Figure 6. The effect of lowering the background current (lower trace) and increasing the inward $Ca^{++}$ ion flow (upper trace) on action potential configuration.

OP-intoxication of cardiac tissue produces modulation of ionic membrane currents that in turn affects the action potential. Using high performance computer experiments, variation in ion channel conductivities were used to gauge the effect on the magnitudes of membrane currents and the action potential. Emphasis was placed on processes thought to influence LQT, a precursor to VF and SCD. Acquired LQTS is characterized by prolongation of the repolarization period that may be the precursor to processes leading to sudden cardiac death.

Reduction of the repolarization currents mimics the genetically caused loss of function in congenital LQT. Reduction in the conductivity of the potassium channels (reduced channel density) or an inactivation of the sodium gate allowing a persistent late current of only 0.1% of peak, prolongs the APD and mimics LQT3, a defect in the sodium channel.

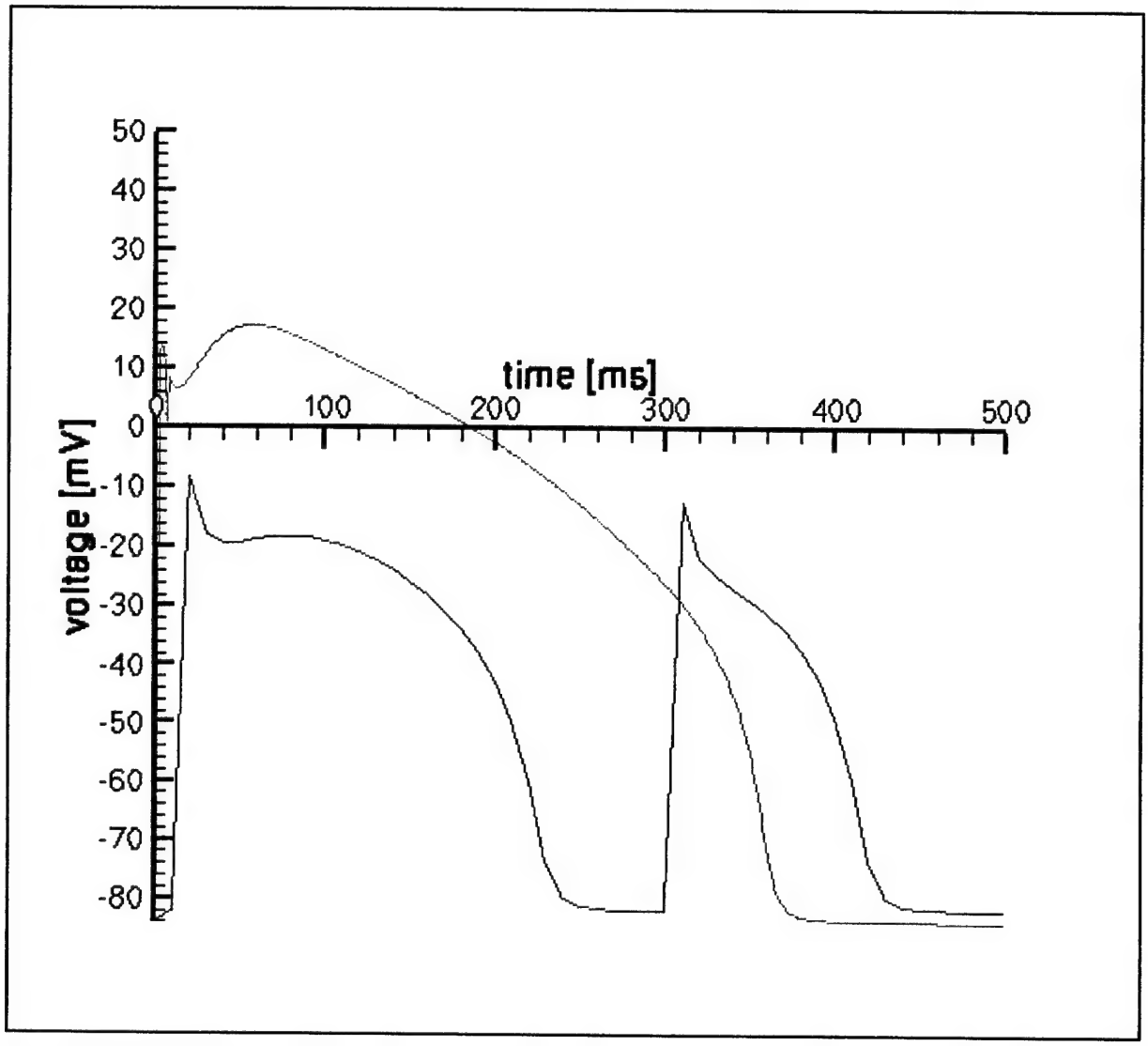


Figure 7. With high background current ($Na^+$ and $Ca^{++}$), the action potential does not reach the overshoot domain. The second stimulus, of the same magnitude, has a considerably shortened cycle length. The baseline action potential (top trace) is shown in green.

One of the underlying assumptions was that OP-induced ACh overload results in patches of tissue with $[K^+]_0$ in excess of normal values. When an action potential encounters such a region, reentry can occur. Conditions were sought by modulation of membrane currents that could block reentry. This is important, since it is believed that the morphology of VF is a progression from tachycardia, through the breakup of spiral waves in the tissue, to fibrillation.

There is considerable uncertainty on the ion channel conductivity values that are species specific and variable even within the same organ. In interpreting the results, the emphasis is on the trends and not on absolute values.

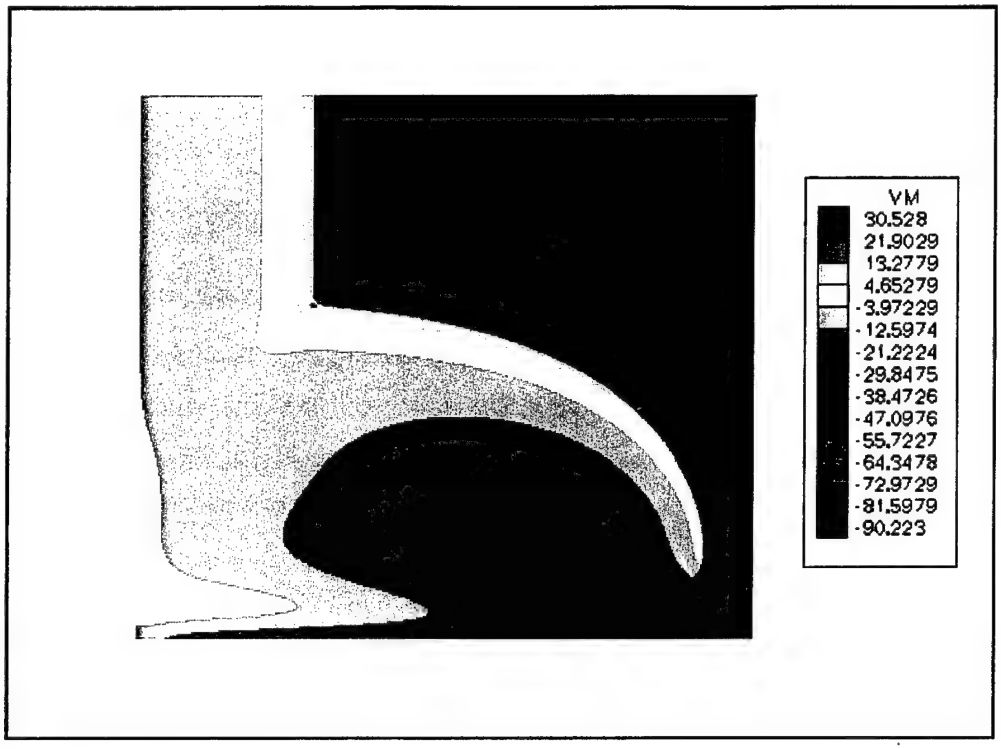


Figure 8. The effect of the interaction of two waves running perpendicularly, with the second started at 425 ms.

These simulations reproduced a number of the observed AP changes in vivo and provide insights to the requirements on the properties of antidotes for OP poisoning.

These calculations suggest that, in addition to the blocking of ACh, the OP ligand interferes with the ion channels, changing the magnitude of currents. In addition, the results demonstrate that modulation of membrane currents, by blocking some of the potassium channels, favors processes leading to reentry. $K^+$, that is $I_{K(ATP)}$ channel openers such as nicorandil, shorten the QT interval and APD, and suppress EAD and thus TdP. Further research is still needed along these lines though since $K^+$ channel openers lower the blood pressure and may be arrhythmogenic. Potassium infusion [19] has been shown to abbreviate the QT interval in LQT2 patients with an $I_{Kr}$ defect.

Based on the insights from these computer experiments, the challenge for devising therapeutics for force protection is to formulate an antidote that acts as a channel opener by increasing potassium currents, lowers calcium accumulation within the cell, reverses acidosis, i.e., $H^+$ overload, and also affects the rate of flow of sodium ions. We have made suggestions that meet these criteria.

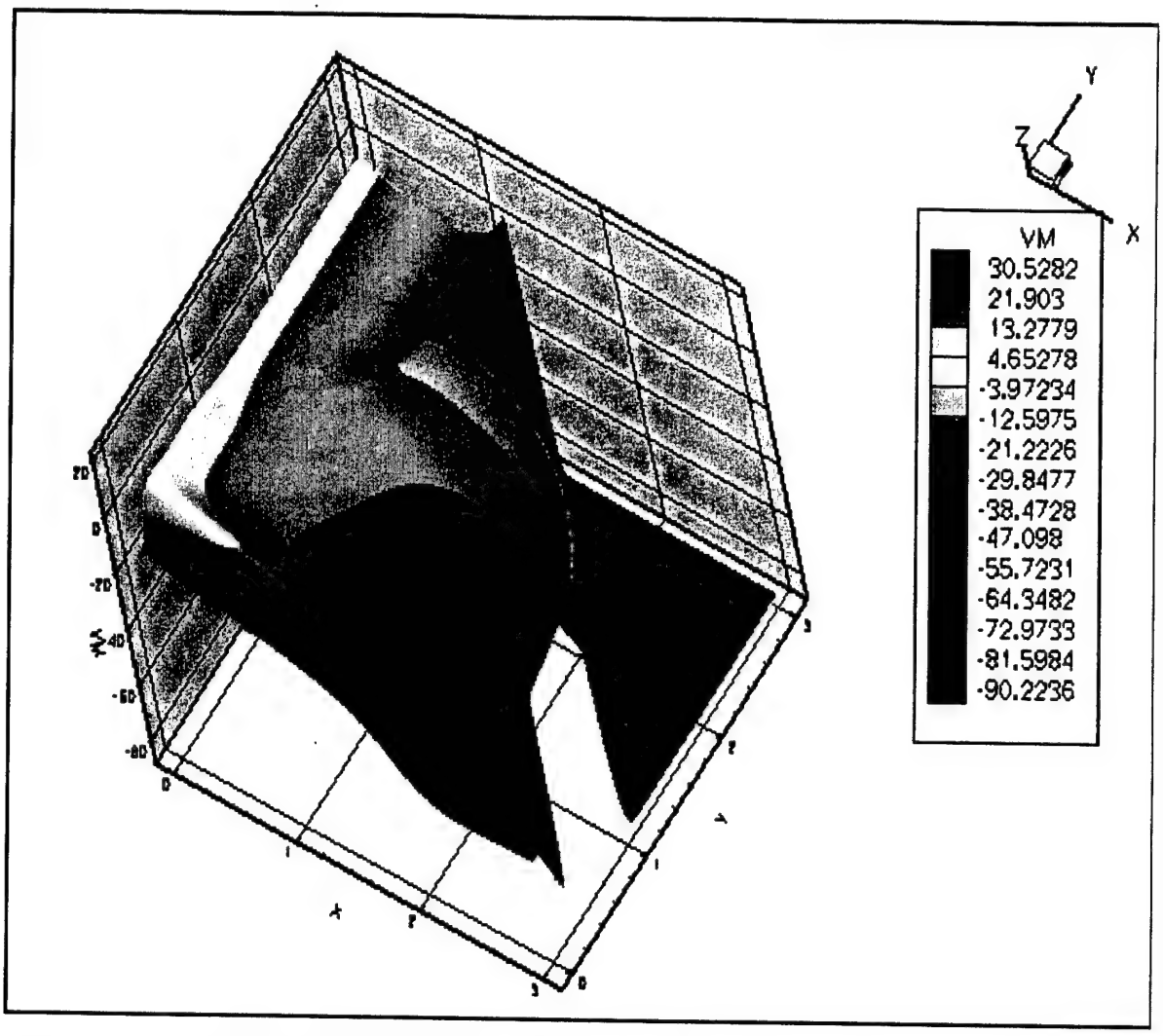


Figure 9. A three-dimensional plot of the action potential at t = 500 ms showing the development of the reentry.

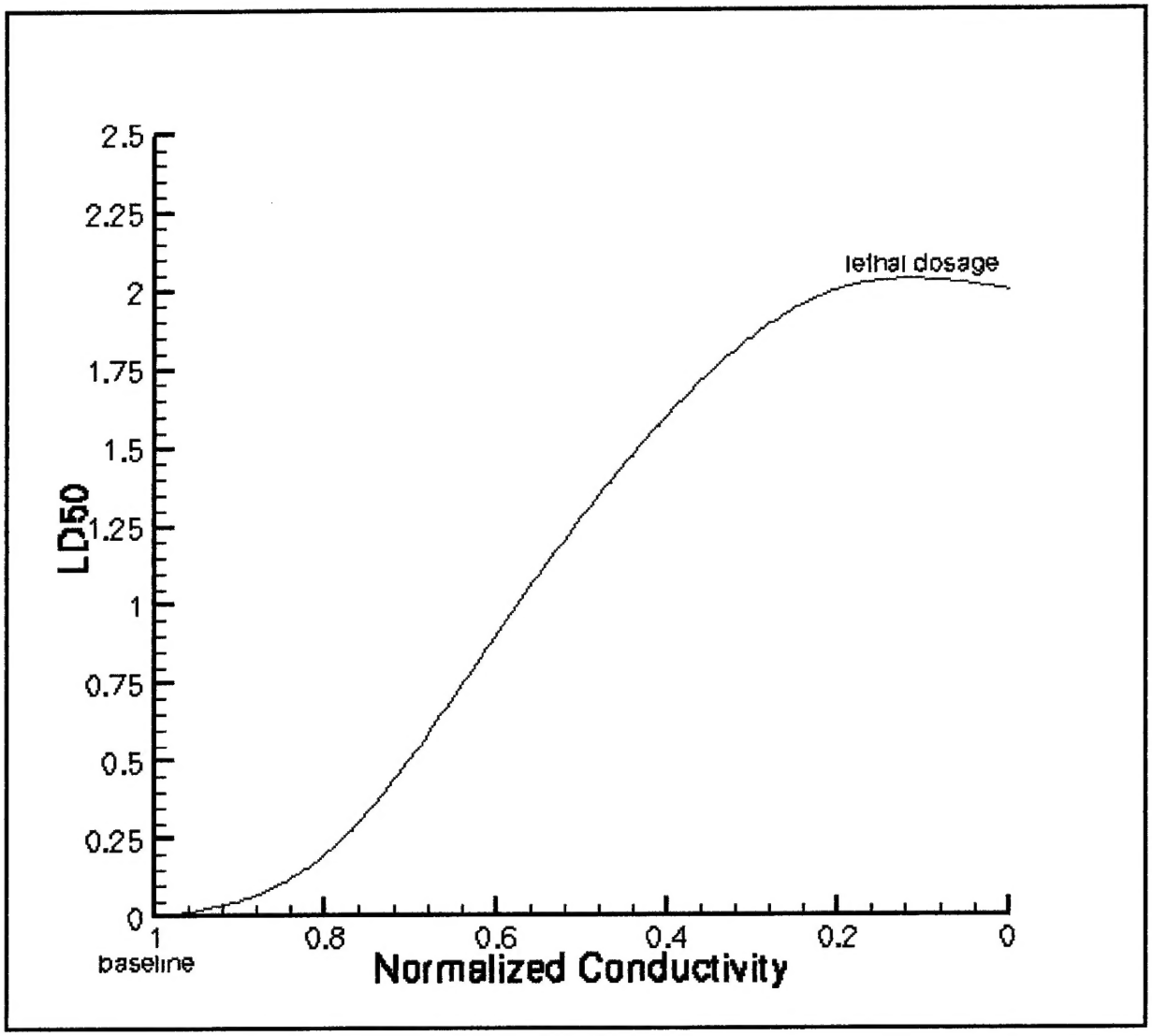


Figure 10. Estimated dose-response curve based on the effect of the lengthening of the cycle due to the presence of the OP in the virtual tissue.

## 6. References


1. Duysen, E. G., B. Li, W. Xie, L. M. Schopfer, R. S. Anderson, C. A. Broomfield, and O. Lockridge. "Evidence for Nonacetylcholinesterase Targets of Organophosphorus Nerve Agent: Supersensitivity of Acetylcholinesterase Knockout Mouse to VX Lethality." *Journal of Pharmacology and Experimental Therapeutics,* vol. 299, pp. 528–535, 2001.

2. Saiyed, H. N., S. K. Gupta, J. P. Jani, and S. K. Kashyap. "Cardiac Toxicity in Pesticide Formulators Exposed to Organophosphate Insecticides." *Indian Journal of Medical Research,* vol. 80, pp. 494–498, 1984.

3. Kiss, Z., and T. Fazekas. "Arrhythmias in Organophosphate Poisonings." *Acta Cardiol,* vol. 34, pp. 323–330, 1979.

4. Ludomirsky, A., H. Klein, P. Sarelli, B. Becker, S. Hoffman, U. Taitelman, J. Barzilai, R. Lang, D. David, E. DiSegni, and E. Kaplinsky. "QT Prolongation and Polymorphous (Torsade de Pointes) Ventricular Arrhythmias Associated to Organophosphorous Insecticide Poisoning." *American Journal of Cardiology,* vol. 49, pp. 1654–1658, 1982.

5. Bar-Meir, A., A. Grubstein, S. Giv'oni, and B. Tadmor. "Cardiac Manifestation of Organophosphate Intoxication." *Harfuah,* vol. 140, pp. 764–769, 2001.

6. Baskin, S. I., and M. P. Whitmer. "The Cardiac Toxicology of Organophosphorus Agents." *Cardiac Toxicology*, edited by S. I. Baskin, Boca Raton, FL: CRC Press, 1991.

7. Roth, A., I. Zellinger, M. Arad, and J. Atsmon. "Organophosphates and the Heart." *Chest*, vol. 103, pp. 576–582, 1993.

8. Hassler, C. R., R. R. Moutvic, D. B. Stacey, and M. P. Hagerty. "Studies of the Action of Chemical Agents on the Heart." AD-A209 219, U.S. Army Medical Research and Development Command, Fort Detrick, MD, 1988.

9. Viskin, S. "Long QT Syndromes and Torsade de Pointes." *Lancet*, vol. 354, pp. 1625–1633, 1999.

10. Antzelevitch, C., and W. Shimizu. "Cellular Mechanisms Underlying the Long QT Syndrome." *Current Opinion in Cardiology*, vol. 17, pp. 43–51, 2002.

11. Jackman, W. M., K. J. Friday, J. L. Anderson, E. M. Aliot, M. Clark, and R. Lazzara. "The Long QT Syndromes: A Critical Review, New Clinical Observations, and a Unifying Hypothesis." *Progress in Cardiovascular Diseases*, vol. 31, pp. 115–172, 1988.

12. Zeng, J., K. R. Laurita, D. S. Rosenbaum, and Y. Rudy. "Two Components of the Delayed Rectifier $K^+$ Current in Ventricular Myocytes of the Guinea Pig Type: Theoretical Formulation and their Role in Repolarization." *Circulation Research,* vol. 77, pp. 140–152, 1995.

13. Viswanathan, P. C., R. M. Shaw, and Y. Rudy. "Effects of $I_{Kr}$ and $I_{Ks}$ Heterogeneity on Action Potential Duration and its Rate Dependence." *Circulation,* vol. 99, pp. 2466–2474, 1999.

14. Liu, D. W., and C. Antzelevitch. "Characteristics of the Delayed Rectifier Current ($i_{Kr}$ and $i_{Ks}$) in Canine Ventricular Epicardial, Midmyocardial, and Endocardial Myocytes." *Circulation Research,* vol. 76, pp. 351–365, 1995.

15. Carmeliet, E. "Cardiac Ion Currents and Acute Ischemia: From Channels to Arrhythmias." *Physiological Review,* vol. 79, pp. 917–1017, 1999.

16. Henning, R. J., and D. R. Sawmiller. "Vasoactive Intestinal Peptide: Cardiovascular Effects." *Cardiovascular Research,* vol. 49, pp. 27–37, 2001.

17. Luo, C. H., and Y. Rudy. "A Dynamic Model of the Cardiac Ventricular Action Potential." *Circulation Research,* vol. 74, pp. 1071–1096, 1994.

18. Nitta, J., T. Furukawa, F. Marumo, T. Sawanobori, and M. Hiraoka. "Subcellular Mechanism for $Ca^{++}$-Dependent Enhancement of Delayed Rectifier $K^+$ Current in Isolated Membrane Patches of Guinea Pig Ventricular Myocytes." *Circulation Research,* vol. 74, pp. 96–104, 1994.

19. Choy, A. M., C. C. Lang, D. M. Chomsky, G. H. Rayos, J. R. Wilson, and D. M. Roden. "Normalization of Acquired QT Prolongation in Humans by Intravenous Potassium." *Circulation,* vol. 96, pp. 2149–2154, 1997.

# Report Documentation Page

*Form Approved*
*OMB No. 0704-0188*



| 1. REPORT DATE *(DD-MM-YYYY)* | 2. REPORT TYPE | 3. DATES COVERED (From - To) |
|---|---|---|
| February 2003 | Final | April–September 2002 |

**4. TITLE AND SUBTITLE**
Computer Study of the Ionic Mechanisms of Organophosphorous-Caused Long-QT Syndrome (LQTS)

**5a. CONTRACT NUMBER**

**5b. GRANT NUMBER**

**5c. PROGRAM ELEMENT NUMBER**

**6. AUTHOR(S)**
Csaba K. Zoltani and Steven I. Baskin*

**5d. PROJECT NUMBER**
2U5/NC

**5e. TASK NUMBER**

**5f. WORK UNIT NUMBER**

**7. PERFORMING ORGANIZATION NAME(S) AND ADDRESS(ES)**
U.S. Army Research Laboratory
ATTN: AMSRL-CI-HC
Aberdeen Proving Ground, MD 21005-5067

**8. PERFORMING ORGANIZATION REPORT NUMBER**
ARL-TR-2902

**9. SPONSORING/MONITORING AGENCY NAME(S) AND ADDRESS(ES)**

**10. SPONSOR/MONITOR'S ACRONYM(S)**

**11. SPONSOR/MONITOR'S REPORT NUMBER(S)**

**12. DISTRIBUTION/AVAILABILITY STATEMENT**
Approved for public release; distribution is unlimited.

**13. SUPPLEMENTARY NOTES**
*U.S. Army Medical Research Institute of Chemical Defense, 3100 Ricketts Point Rd., Aberdeen Proving Ground, MD 21010-5400

**14. ABSTRACT**
An important clinical marker of organophosphorous (OP)-caused cardiac toxicity is long-QT syndrome, the prolongation of the repolarization period in the ventricles, as measured in an electrocardiogram. The primary membrane currents responsible for this condition are two potassium currents, $I_{Kr}$ and $I_{Ks}$. This computer simulation investigated the effect of the modulation of the membrane currents most likely affected by the OP on the action potential in a two-dimensional slab of cardiac tissue. We have shown that modulation and reduction of the potassium currents, changes in the background current, and calcium overload of the cells mimic the experimentally observed change in slope of the depolarization in the presence of OPs as well as the prolongation and change in the shape of the plot of repolarization voltage vs. time. These changes are precursors to the onset of Torsade de Pointes and ventricular fibrillation and suggest the required pharmacology of antidotes for force protection. Based on these results, an estimated dose-response curve is presented.

**15. SUBJECT TERMS**
high performance computing, cardiac toxicity, organophosphorous

| 16. SECURITY CLASSIFICATION OF: | | | 17. LIMITATION OF ABSTRACT | 18. NUMBER OF PAGES | 19a. NAME OF RESPONSIBLE PERSON |
|---|---|---|---|---|---|
| a. REPORT | b. ABSTRACT | c. THIS PAGE | | | Csaba K. Zoltani |
| UNCLASSIFIED | UNCLASSIFIED | UNCLASSIFIED | UL | 28 | 19b. TELEPHONE NUMBER *(Include area code)* (410) 278-6650 |

**Standard Form 298 (Rev. 8/98)**
**Prescribed by ANSI Std. Z39.18**